Regional Cerebral Blood Flow Response to Oral Amphetamine Challenge in Healthy Volunteers

Michael D. Devous, Sr., Madhukar H. Trivedi, and A. John Rush

Nuclear Medicine Center and Departments of Radiology and Psychiatry, University of Texas Southwestern Medical Center, Dallas, Texas

Functional brain imaging is a powerful tool for examining the central nervous system (CNS) response to pharmacologic challenges. Amphetamine is of interest both because of its role as a stimulant of the dopaminergic system and because of its use to alter mood in mood-disordered patients, particularly in patients suffering from depression. In this study, we report the effects of oral d-amphetamine relative to placebo on regional cerebral blood flow (rCBF) measured by SPECT in healthy volunteers to characterize the normal CNS response to this primarily dopaminergic stimulant. **Methods:** SPECT was used to assess changes in rCBF induced by amphetamine in 16 healthy volunteers. Subjects received placebo and then 0.4 mg/kg oral amphetamine in a fixed-order single-blind design and were imaged on a triple-head tomograph. Another six healthy volunteers received placebo at both times to assess normal rCBF variability. rCBF changes were assessed with a three-dimensional voxel-based analysis integrated into an automated coregistration system. Data were automatically normalized to whole-brain counts and coregistered. Resultant rCBF changes were evaluated parametrically through the formation of an image whose voxel values were based on the paired *t* statistic. **Results:** Amphetamine increased rCBF in two mesial prefrontal zones (Brodmann's areas 8 and 10), inferior orbital frontal lobe (area 11), brain stem (ventral tegmentum), anteromesial temporal lobe (amygdala), and anterior thalamus. Amphetamine decreased rCBF to motor cortex, visual cortex, fusiform gyrus, posterolateral temporal lobe, and right lateral temporal lobe. **Conclusion:** Our data suggest that amphetamine induces focal increases and decreases in rCBF in healthy volunteers in areas primarily innervated by dopamine pathways and in areas with secondary (primarily limbic) affiliations. These data are consistent with glucose metabolic data from autoradiographic studies in animals, in which the largest increases are seen in brain stem, followed by striatum, thalamus, and frontal and sensory cortices. Frontopolar and temporal increases observed in our study appear to be unique to humans.

Key Words: amphetamine challenge; rCBF; SPECT; healthy volunteers

J Nucl Med 2001; 42:535–542

Functional or biochemical central nervous system (CNS) pathology has historically been inferred by measurements of precursors or metabolites in cerebrospinal fluid, plasma, platelets, or urine under resting conditions (*1*). However, passive measurement strategies have been successfully supplemented by pharmacologic, motoric, or cognitive challenge studies in which the CNS is perturbed and its chemical, psychologic, or endocrinologic response is measured. In vivo challenge studies, together with in vitro neurochemical results, have provided clues to the possible locus and nature of various CNS abnormalities. These strategies may help to differentiate within and among disorders affecting the CNS and to establish the biologic profiles of diagnostic subtypes.

CNS changes during an amphetamine challenge may be particularly informative because dopaminergic, noradrenergic, and serotonergic mechanisms have been implicated both in the action of amphetamines and in several psychiatric disorders, including depression and schizophrenia. Amphetamine has already been used as a challenge test in the study of depression to determine behavioral (*2–5*) and neuroendocrine (*6,7*) responses and to predict treatment response (*8,9*). Amphetamine has also been used in schizophrenic patients to determine behavioral responses (*8–10*), neuroendocrine responses (*11*), responses to psychotherapeutic agents (*12–14*), and the probability of relapse (*11,15*).

Simultaneous with the emergence of challenge strategies in psychiatric research, in vivo imaging of brain function by SPECT or PET has provided evidence, with neuroanatomic specificity, of abnormal CNS function in most psychiatric disorders (*16–17*). Maturation in the technology of SPECT regional cerebral blood flow (rCBF) imaging has substantially expanded the potential for complex, detailed studies of brain function. New tomographs (including that used for these studies) produce three-dimensional rCBF images of 6- to 8-mm spatial resolution. Developments in image analysis now permit routine coregistration of image sets created under different conditions in a single subject or of images from groups of subjects. Such techniques in combination with voxel-based statistical analyses ("*t* images" or "*z* im-

ages") greatly enhance the assessment of change in functional images and the diversity of information derivable from challenge experiments. SPECT also has the advantage of snapshot radiopharmaceuticals that permit tracer administration remote from the scanner in an environment where visual, auditory, and somatosensory stimuli can be controlled or manipulated for experimental purposes.

It is thus a natural course to combine functional brain imaging by PET or SPECT with pharmacologic challenges in the study of CNS disorders. In this study, we report the effects of a 0.4 mg/kg oral dose of d-amphetamine relative to placebo on rCBF measured by SPECT in healthy volunteers to characterize the normal CNS response to the administration of d-amphetamine.

MATERIALS AND METHODS

Subjects

Twenty-two healthy volunteers (14 men, 8 women; age range, 24–40 y) provided written informed consent for this investigation according to the guidelines of the Institutional Review Board of the University of Texas Southwestern Medical Center. They were part of a large healthy control pool maintained by the Mental Health Clinical Research Center recruited by advertising and by word of mouth. The subjects were evaluated medically, with a thorough review of medical systems and laboratory screening tests, including complete blood cell count with differential; urinalysis; microscopic urinalysis; T3, T4, and T3-RIA; SMA 20; and toxicology screens. Subjects were excluded if they had a history of significant head trauma, loss of consciousness, seizure disorder, transient ischemic attacks, or other significant neurologic disorders or major medical disorders (e.g., hypertensive, cardiac, pulmonary, endocrinologic, gastrointestinal, or autoimmune). In addition, the subjects were required to be completely free of past or present axis I psychiatric disorders as determined by the Structured Clinical Interview for DSM-III-R (18) (*Diagnostic and Statistical Manual of Mental Disorders, Third Edition, Revised*) and a thorough psychiatric interview; any concurrent or past major medical problems; and a family history of depression, suicide, alcoholism, schizophrenia, Alzheimer's disease, or other major psychopathology in all first-degree relatives. Subjects with a contraindication to amphetamine (e.g., a history of arrhythmias or hypertension) were also excluded, as were subjects with a diastolic pressure > 90 mm Hg or a systolic pressure > 150 mm Hg. The subjects were medication free for at least 14 d and had not used alcohol for the last 7 d.

Experimental Protocol

Sixteen subjects were studied by SPECT rCBF imaging under placebo and amphetamine challenge states, and an additional six subjects were studied in the placebo state twice to establish the null set response. Eleven subjects (six placebo–placebo and five placebo–amphetamine) were studied in a single half-day session using dual-isotope imaging (19,20). When ¹²³I-iodoamphetamine (IMP) became unavailable, an additional 11 placebo–amphetamine subjects were studied in a two-day protocol, with each imaging session separated by 48 h to ensure complete removal of ⁹⁹ᵐTc background from the first study. For both the 1-d and the 2-d protocols, placebo and then amphetamine (0.41 ± 0.06 mg/kg) were administered orally in identical capsules in a single-blind

fixed-order design. This approach, rather than a double-blind random-order design, was chosen so that the subjects would not be aware of whether placebo or amphetamine was being administered and to simultaneously ensure that any lasting effects of amphetamine could not affect the placebo images.

The subjects were first seated in a dimly lit room with their eyes and ears open. Then, a 22-gauge Quik-Cath needle (Baxter Healthcare Corp., Deerfield, IL) was inserted into a forearm vein (nondominant arm) and connected to polyethylene tubing extending outside the subject's field of view for remote administration of radiotracers. A slow intravenous drip of normal saline was used to maintain an open vein. After a 10-min accommodation period, baseline vital signs were obtained. rCBF tracers were administered 75 min after placebo or amphetamine. Tracer administration was specifically timed to occur at peak motor and cognitive responses to amphetamine (3,6,10). Scanning occurred in the last 40 min of the experimental period.

One-Day Protocol. For the 1-d, dual-isotope protocol, oral placebo was given after baseline measures, with the subject unaware of which compound was being given. ⁹⁹ᵐTc-hexamethylpropyleneamine oxime (HMPAO; 740 MBq) was injected 75 min later. Amphetamine was given at 95 min, and IMP (111–222 MBq) was injected 75 min after amphetamine administration. At 20 min after IMP, the intravenous line was removed and the subject was positioned supine in the scanner (PRISM 3000S, Picker, Cleveland, OH). Dual-isotope SPECT scanning ensued for 40 min. Final vital signs were obtained after scanning. The dual-isotope technique, described in detail by Devous et al. (19,20), permits simultaneous imaging of the distribution of ⁹⁹ᵐTc-HMPAO and ¹²³I-IMP to monitor changes in rCBF occurring after the initial tracer injection.

Two-Day Protocol. For the two-day single-isotope protocol, the oral placebo was given after baseline measures as described above. ⁹⁹ᵐTc-HMPAO (740 MBq) was injected 75 min later. At 20 min after HMPAO, the intravenous line was removed and the subject was positioned in the scanner. Conventional SPECT scanning ensued for 20 min. After scanning, final vital signs were assessed. The subject returned to the laboratory after 48 h and the procedure was repeated, except that amphetamine was given instead of placebo.

rCBF Imaging

⁹⁹ᵐTc-HMPAO was prepared from the lyophilized kit per package insert instructions, with technetium pertechnetate eluted no more than 1 h before use. Seven hundred forty megabecquerels of labeled compound, withdrawn from reconstituted kits no more than 20 min after reconstitution, and 111–222 MBq ¹²³I-IMP obtained in the labeled form, were administered to the subject.

For the 1-d protocol, high-resolution fanbeam collimators were positioned 13 cm from the axis of rotation and projection data were acquired in a 128 × 128 matrix in 3° increments for 40 min using two windows: for ⁹⁹ᵐTc, a 15%-wide centered window; for ¹²³I, a 10%-wide asymmetric window, beginning at the middle of the photopeak. These windows have been shown (19,20) to provide less than 5% cross-contamination of the two isotopes. Rapid acquisition sequencing was used for all acquisitions, which permits 360° sampling in 5-min increments. When acquisition was complete, the eight 5-min scans were summed and treated as a single acquisition. For the 2-day protocol, ⁹⁹ᵐTc-HMPAO was prepared as described above and acquisition was conducted in the same way, except that the ⁹⁹ᵐTc window was widened to 20%, no ¹²³I window was used, and the scan was shortened to 20 min.

Image reconstruction was performed in the transverse domain using backprojection with a ramp filter. To match IMP and HMPAO image resolution, the cutoff frequency for a sixth-order Butterworth filter was selected for both IMP and HMPAO from the power spectrum of Fourier transformed transverse images for IMP (the limiting case), so that the tail of the filter crossed the high-frequency end of the image power spectrum at the 10% amplitude level (*19–20*). These parameters were then applied to all image sets (^{123}I and ^{99m}Tc). For our system, voxels in reconstructed images were 1.9 mm^3. After reconstruction, images were attenuation corrected, using a Chang first-order method.

Image Analysis

Image analysis consisted of three components: image normalization, image coregistration, and three-dimensional paired-*t* statistical analysis. Intrasubject normalization of image count density corrects for the difference in administered dose between two sessions and for differences in global cerebral blood flow across conditions. This was accomplished by normalizing counts in each voxel to whole-brain count density for each subject in both the placebo and the amphetamine datasets. Then, a ratio of whole-brain count density between placebo and amphetamine datasets was computed for each subject, and the resultant placebo–amphetamine count ratio was then used as a scaling factor to equate global count density in amphetamine images to that in the placebo images. Intersubject normalization (correcting for global variability in tracer uptake between subjects) was accomplished at the same time as intrasubject normalization by first scaling whole-brain counts in the placebo data to 100. Thus, when normalization was completed, whole-brain count density for both placebo and amphetamine conditions for all subjects had a value of 100, yielding both intra- and intersubject normalized images. We chose the whole brain for count normalization rather than the cerebellar counts used by some investigators because some animal data (*21,22*) and our data suggest an effect of amphetamine on cerebellar gray matter.

Image sets were next coregistered within or between subjects to the coordinate system of Talairach and Tournoux (*23*) using a modified version of the coregistration algorithm of Pelizzari et al. (*24*) integrated with an automated analysis system for SPECT brain images. Data are automatically resliced to 2-mm^3 voxels, normalized, and coregistered. A final visual check by the operator is used to validate the coregistration.

Our analyses use three-dimensional paired *t* images as representative of the change in level of the different group means. The distribution of *t* values across all voxels is mapped, and a threshold based on the *t* value at the $P < 0.05$ level for the number of degrees of freedom of the experiment is used to identify voxels participating in the response to amphetamine. Because these voxels represent both real responses and random parts of the null set *t* distribution, we search the *t* image voxels for a neighborhood association. We assume that voxels from the null set *t* distribution will be randomly distributed in space and so can be removed by requiring that "acceptable" voxels have neighbors that also meet the selected *t* threshold. Remaining significant voxels are next mapped onto a model brain to produce a parametric statistical image that identifies response location. The final *t* image reveals those voxels whose relative rCBF differed most between the placebo and the amphetamine states relative to the inherent variability of each voxel, thus minimizing artifacts caused by differences in anatomy, physiology, and image processing. The result is an image of anatomic zones (e.g., regions of interest) that contribute to significant rCBF responses to amphetamine, the boundaries of which are defined by the data.

RESULTS

Placebo–Placebo Studies

A subset of six subjects received placebo on both occasions to establish the null set response. No changes in hemodynamic parameters were noted in placebo–placebo studies. Images of attenuation-corrected 128 × 128 1.9-mm-thick transverse sections from a single subject using the dual-isotope technique are shown in Figure 1. To evaluate image normalization procedures, we compared intrasubject scaling factors for the whole brain, centrum semiovale (white matter), and cerebellar regions of interest in these six subjects. Scale factors based on whole brain and centrum-semiovale did not differ within subjects (Fig. 2). However, cerebellum-based scale factors were uniformly higher (HMPAO > IMP; 19% ± 3%), confirming an earlier report (*25*) that cerebellar uptake relative to cortical or subcortical uptake is greater for ^{99m}Tc-HMPAO than for ^{123}I-IMP. This finding provides additional evidence against using the cer-
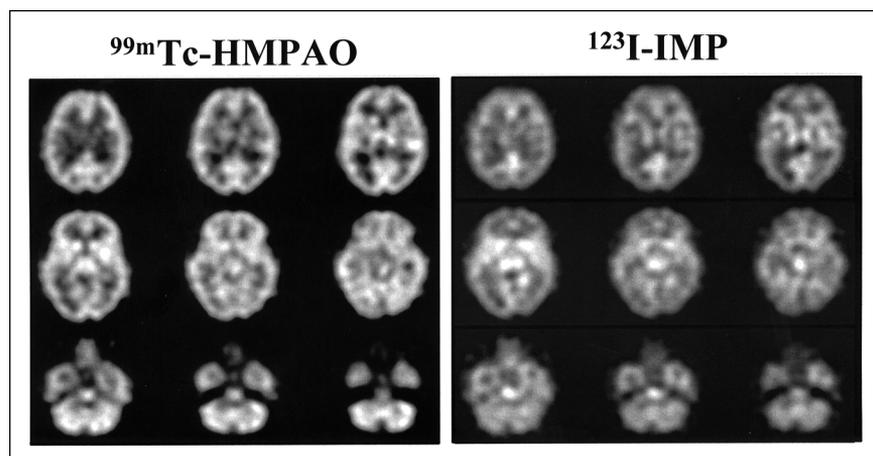
FIGURE 1. Typical ^{99m}Tc-HMPAO and ^{123}I-IMP images using dual-isotope technique in placebo–placebo healthy volunteer illustrates resolution of such images from PRISM tomograph using dual-isotope acquisition technique. These attenuation-corrected, 128 × 128, 1.9-mm-thick transverse images were ramp reconstructed and postfiltered, with Butterworth sixth-order filter adjusted to match amplitude of IMP power spectrum. For this figure, images were then averaged three slices to one for final slice thickness of 6 mm.
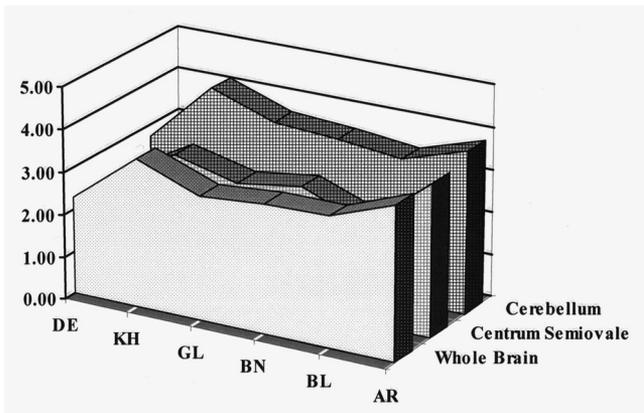
FIGURE 2. Comparisons of relative distribution of HMPAO to that of IMP among cerebellum, whole brain, and centrum semiovale (white matter) for six placebo–placebo healthy volunteers. Whole-brain and centrum semiovale HMPAO/IMP ratios are essentially identical for all six subjects, whereas cerebellar uptake ratios are consistently higher (19% ± 3%).

ebellum for count normalization when comparing data obtained from HMPAO and IMP.

Other than residual cerebellar activity, no consistent areas of difference were found between HMPAO and IMP images. We also compared circumferential region-of-interest count densities from the coordinate-transformed, normalized images averaged over the six placebo–placebo controls (Fig. 3). The data were linearly correlated ($r = 0.93$), the slope did not differ from 1, and the intercept did not differ from 0.

Placebo–Amphetamine Studies

Hemodynamic Response. Hemodynamic changes after amphetamine were rare. Mild blood pressure and pulse elevations were seen in 3 subjects (peak at 120 min), whereas 14 subjects showed no changes in vital signs.

rCBF. t images showing areas of increased rCBF after amphetamine challenge in 16 placebo–amphetamine subjects are presented in Figures 4 (transverse images) and 5
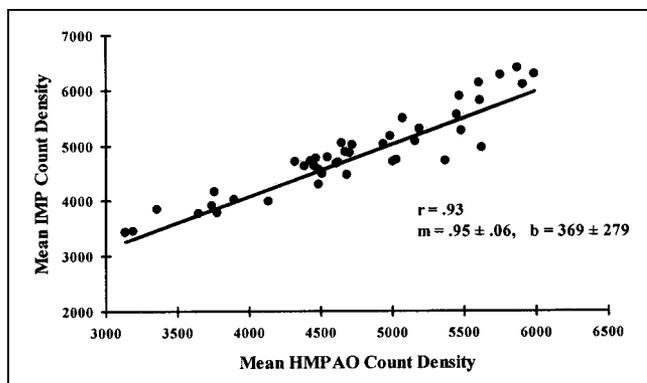
FIGURE 3. Comparison of relative distributions for IMP and HMPAO within identical cortical region of interest in six placebo–placebo healthy volunteers indicates colinear distributions in resting subjects.

(sagittal images). Areas of significant change (median-filtered voxels lying above or below the $t = \pm 2.20$ threshold in the t distribution) are shown as solid white objects overlaid on the model brain, to which all images were coregistered. As seen in Figure 4, rCBF was increased bilaterally after amphetamine in two mesial prefrontal zones (Brodmann's areas 10 and 8), brain stem (ventral tegmentum), anteromesial temporal lobe (amygdala), and anterior thalamus. Inferior orbital frontal activation (Brodmann's area 11) was also seen (not shown in Fig. 4).

No unilateral changes were seen, although the subcortical response was larger in t-value magnitude and extent on the right, whereas the amygdala response was larger on the left. t-value magnitude reflects the strength of the statistical response and can be a consequence of greater rCBF change, decreased variability among subjects, or both. Areas of maximum change are identified in Table 1 by Talairach coordinates (response centroid, in millimeters). The Talairach coordinates are shown as positive to the right of, and anterior and superior to, the anterior commissure.

Areas of decreased rCBF after amphetamine are shown as sagittal images in Figure 5. Decreased rCBF after amphetamine in healthy volunteers involved fewer locations but similar t magnitude. A small decrease was seen in the motor cortex (Brodmann's area 6), visual cortex, fusiform gyrus, and posterolateral temporal lobe (left greater than right). Decreases were also observed in the right lateral temporal lobe extending superiorly toward Sylvius' fissure. Talairach coordinates for the decreases are shown in Table 2.

DISCUSSION

Amphetamine affects at least three neurotransmitter systems: dopamine, norepinephrine, and serotonin (26–30). Most of the CNS effects of amphetamine are thought to be of dopaminergic origin. Amphetamine increases the concentrations of both dopamine and norepinephrine at the synapse by blocking reuptake and stimulating release (31), decreases the uptake of ^{3}H-dopamine in the corpus striatum (32), and depresses spontaneous firing rates of dopamine-producing cells in the substantia nigra (26). Similar effects are observed in norepinephrine systems (26–27). Thus, one might expect areas of both increased and decreased rCBF after an amphetamine challenge.

Where one might expect such rCBF changes is based on the innervation of these neurotransmitter systems. The relevant receptor systems—interdigitate striatum, cortex (especially prefrontal cortex), and limbic systems—are likely related to three primary circuits (33–34). The first is the dorsolateral prefrontal circuit, which includes Brodmann's areas 9 and 10 in a closed loop with subcortical structures and areas 46, 8, and 7 as open afferents and efferents, as well as components of the thalamus, striatum, substantia nigra, and ventral tegmentum. The second is the lateral orbital frontal circuit, which includes the medial aspect of area 10; area 11 in the closed loop; areas 12, 22, 25, and 32
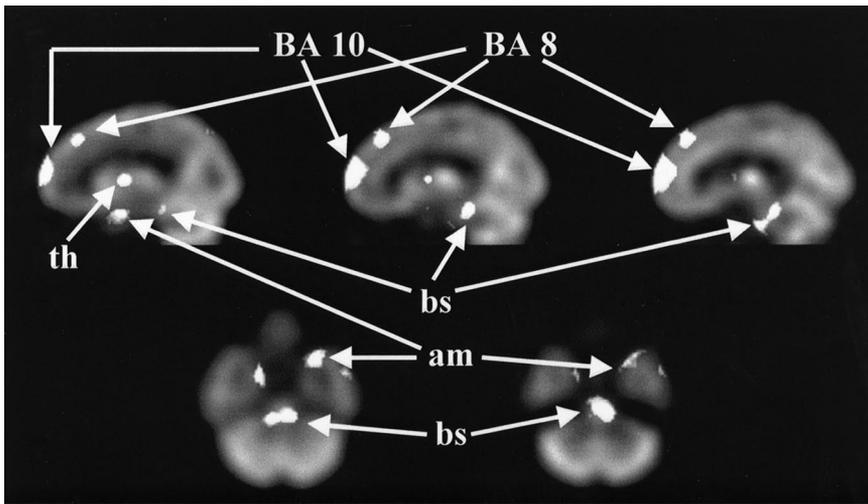
FIGURE 4. Sagittal and transverse images show areas of increased rCBF after amphetamine challenge. Areas of significant change (identified as median-filtered voxels lying above $t = 2.20$ threshold in t distribution) are shown as solid white objects overlaid on model brain to which all images are coregistered. Images are oriented with subject's left on viewer's right. Brodmann's areas (BA) are designated by number. am = anteromesial temporal lobe (amygdala); bs = brain stem; th = anterior thalamus.

as open aspects; and, subcortically, the thalamus, striatum, substantia nigra, amygdala, and ventral tegmentum. Afferents from the entorhinal cortex and efferents from the anterior cingulate and the temporal pole also are involved (*34*). The third circuit is the anterior cingulate, or limbic, circuit, which includes Brodmann's area 24 (anterior cingulate), the hippocampus, and the entorhinal (area 28) and perirhinal (area 35) regions, as well as the ventral striatum, medial orbital frontal cortex, amygdala, thalamus, hypothalamus, subthalamic nucleus, globus pallidus, lateral habenula, and ventral tegmentum (*33*).

The rCBF response to amphetamine observed in our data is consistent with primary activation of the lateral orbital frontal circuit (mesial aspect of Brodmann's areas 10 and 11), partial activation of the anterior cingulate/limbic circuit (amygdala but not anterior cingulate), and activation of only efferent components of the dorsolateral prefrontal cortex circuit (Brodmann's area 8). Activation of ventral tegmentum and anterior thalamus is likely common to all three circuits. Decreased rCBF in area 6 might be a consequence of direct activation of the ventral anterior thalamic nucleus (direct inhibition) or an indirect consequence of activation

of area 8 (which has been shown to be homolaterally connected to area 6 in primates (*23*)), if area 8 has an inhibitory influence on area 6 (not known). Similarly, decreased rCBF in the fusiform gyrus may also be related to inhibitory influences of area 8, which represents a large portion of the frontal oculomotor field. Posterolateral temporal lobe decreases are less readily interpreted.

Dopaminergic systems arising from the midbrain are clustered into the retrorubral field, the substantia nigra, and the ventral tegmentum. Cells arising from the substantia nigra ascend to the striatum, are referred to as the nigrostriatal pathway, contain 70% of brain dopamine, and are primarily involved in the modulation of motor behavior. Neurons ascending from the ventral tegmentum project to limbic and cortical areas (cingulate, entorhinal, prefrontal, and piriform cortices) and are referred to as the mesolimbic and mesocortical pathways, respectively (*35*). The mesolimbic dopaminergic pathway is primarily related to the anterior cingulate (limbic) circuit, whereas the mesocortical pathway relates to the dorsolateral prefrontal and lateral orbitofrontal circuits. Our data are most consistent with involvement of the mesolimbic and mesocortical pathways,
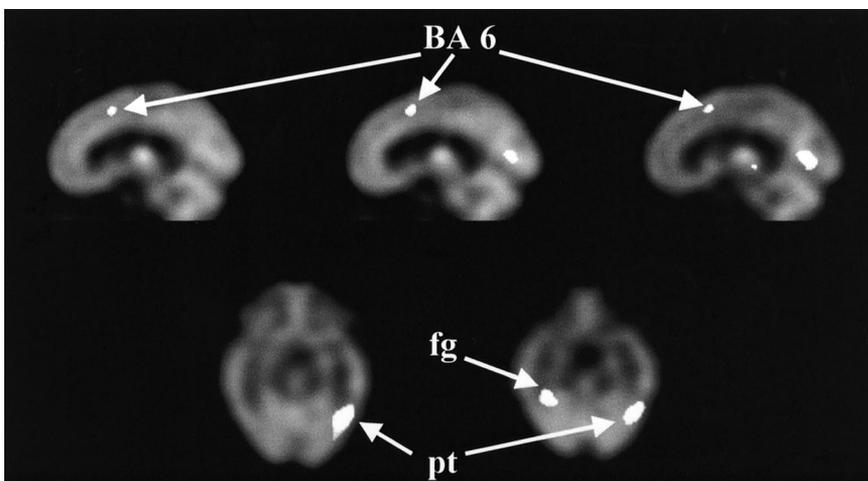
FIGURE 5. Sagittal and transverse images display areas of decreased rCBF ($t \leq -2.20$) after amphetamine. Brodmann's areas (BA) are designated by number. fg = fusiform gyrus; pt = posterolateral temporal lobe.

TABLE 1
Regions of rCBF Increases in Healthy Volunteers After Amphetamine Challenge Referenced to Talairach Coordinates

Region	Brodmann's area 10	Brodmann's area 8	Brain stem	Left amygdala	Anterior temporal region
x, y, z	2, 58, 14	4, 40, 44	−4, −26, −26	−28, 14, −22	−6, −6, 10
maximum t	4.38	2.99	2.46	4.02	2.45

with little evidence of activation of the striatal–nigral pathway.

Extant literature about the metabolic impact of amphetamine on the CNS primarily derives from studies in animals, and three general conclusions can be drawn from that literature: first, that amphetamine causes focal, but not global, changes in rCBF and regional cerebral glucose metabolism (rCGM); second, that rCBF and rCGM remain coupled during an amphetamine challenge (*21,22*); and third, that amphetamine has no direct vascular effects (*21,22*). Specifically, amphetamine increases rCGM in rats in the substantia nigra, subthalamic nucleus, striatum, visual cortex, thalamus, hypothalamus, and frontal and sensory-motor cortices (*21*). Decreased metabolic rates are found in the suprachiasmatic nucleus and habenula. Neither global nor white matter changes are observed. Our data show a striking consistency with these glucose metabolic data in animals: largest increase in the midbrain, followed by the frontal and sensory cortices. The frontopolar and temporal increases and parasagittal and cingulate decreases we observed appear to be unique to humans, and we do not see striatal responses. The lack of striatal response may be dose related. The animal studies were typically conducted at a higher dose than that used in our protocol and at which motor responses related to the striatal–nigral pathway are most activated. Ventral tegmentum activation dominates at lower doses.

The effect of amphetamine on rCBF or rCGM has been reported several times for schizophrenia, once for healthy volunteers, and once for attention deficit hyperactivity disorder. In the first of the studies on schizophrenia, Wolkin et al. (*36*) noted in healthy volunteers ($n = 6$) a significant decrease in rCGM measured by ^{18}F-FDG PET in the left and right frontal and left temporal regions after amphetamine (0.5 mg/kg by mouth), whereas in schizophrenic patients ($n = 10$) only a right temporal metabolic decrease was

TABLE 2
Regions of rCBF Decreases in Healthy Volunteers After Amphetamine Challenge Referenced to Talairach Coordinates

Region	Brodmann's area 6	Visual cortex	Fusiform gyrus	Lateral temporal region
x, y, z	−4, 12, 50	−10, −70, 8	−40, −66, −2	32, −38, −16
maximum t	−5.05	−2.80	−2.21	−3.08

observed. In a follow-up study on 17 schizophrenic patients, these authors (*37*) noted that amphetamine decreased rCGM primarily in the left temporal lobe and increased rCGM in the striatum and cerebellum. The lack of significant increases in the prefrontal and orbitofrontal cortices in these studies contrasts substantially with our data. The most likely explanation for this difference is the time course of radiopharmaceutical uptake. FDG uptake occurs over approximately 30 min, whereas motor and cognitive responses to amphetamine are generally more acute and are delayed in their onset from oral administration. The timing of FDG was not coordinated with subject responses in the studies of Wolkin et al. (*36–37*). ^{99m}Tc-HMPAO uptake is first pass (approximately 15 s from intravenous administration), and IMP uptake occurs over approximately only 2 min, and their administration was specifically timed to occur at peak motor and cognitive responses to amphetamine in our protocol. In this context, both our protocol and our data are more consistent with the animal studies described above.

Daniel et al. (*38*) found increased activation of the dorsolateral prefrontal cortex during the Wisconsin Card Sort task after amphetamine (0.25 mg/kg by mouth) relative to placebo in 10 schizophrenic patients using rCBF by ^{133}Xe SPECT. More recently, this group (*39*) studied the effect of amphetamine on rCBF changes during two abstract reasoning tasks (Wisconsin Card Sort and Raven's Progressive Matrices) relative to a (sensory motor) control task using PET. Amphetamine selectively enhanced rCBF in the hippocampus during the performance of Raven's Progressive Matrices and in the dorsolateral prefrontal cortex during the Wisconsin Card Sort. The authors concluded that amphetamine "focused" neural activity in those areas where it was normally performed and offered this mechanism as an explanation for the ability of amphetamines to improve cognitive efficiency. Enhanced prefrontal activation on the surface seems consistent with our data, but these investigators did not report on the effects of amphetamine on prefrontal rCBF without concurrent cognitive activation, and thus our data are not easily compared.

In 13 adults with attention deficit hyperactivity disorder, Matochik et al. (*40*) found no change in global glucose metabolism (FDG) after an acute 0.25 mg/kg oral amphetamine dose and only small changes in rCGM. In a subsequent study in 8 adults with attention deficit hyperactivity disorder, they (*41*) found no significant changes in either global cerebral glucose metabolism or rCGM after amphet-

amine (0.15 mg/kg intravenously). The lack of regional activation in these studies (as in the rCGM studies of Wolkin et al. (*36,37*) in schizophrenia described above) highlights both technical limitations of current studies and fundamental limitations of FDG PET. Although both studies came from the same group, the amphetamine doses differed by almost a factor of two, and the timing of drug administration versus FDG administration was strikingly different (FDG 90 min after oral amphetamine in the first, 3 min after intravenous amphetamine in the second) and in neither case was gauged to match peak cognitive responses. Again, unless the CNS response has rapid onset and prolonged endurance, the FDG studies we have described will represent the average of times of no response with true responses.

CONCLUSION

Our data, in combination with previous animal and human studies, suggest that amphetamine induces focal increases and decreases in rCBF in healthy volunteers in areas primarily innervated by dopamine pathways and in areas with secondary (primarily limbic) affiliations. These findings are consistent with the animal literature and with the human literature, in which the time course of measurements is similar.

ACKNOWLEDGMENTS

REFERENCES

1. Rush AJ, Cain JW, Raese J, et al. Neurobiological bases for psychiatric disorders. In: Rosenberg RN, ed. *Comprehensive Neurology*. New York, NY: Raven Press; 1991:555–608.

2. Checkley SA, Crammer JL. Hormone response to methylamphetamine in depression: a new approach to the noradrenalin depletion hypothesis. *Br J Psychiatry.* 1977;131:582–586.

3. Silberman EK, Reus VI, Jimerson DC, et al. Heterogeneity of amphetamine response in depressed patients. *Am J Psychiatry.* 1981;138:1302–1307.

4. Langer G, Heinze G, Reim B, et al. Reduced growth hormone responses to amphetamine in "endogenous" depressive patients. *Arch Gen Psychiatry.* 1976; 33:1471–1475.

5. Halbreich U, Sachar EJ, Asnis GM, et al. Growth hormone response to dextroamphetamine in depressed patients and normal subjects. *Arch Gen Psychiatry.* 1982;39:189–192.

6. Fawcett J, Siomopoulos V. Dextroamphetamine response as a possible predictor of improvement with tricyclic therapy in depression. *Arch Gen Psychiatry.* 1971;25:244–247.

7. van Kammen DP, Murphy DL. Prediction of imipramine antidepressant response by a one-day d-amphetamine trial. *Am J Psychiatry.* 1978;135:1179–1184.

8. van Kammen DP, Bunney WE, Docherty JP, et al. Amphetamine-induced catecholamine activation in schizophrenia and depression. In: Costa E, Gessa GL, eds. *Advances in Psychopharmacology.* Vol 16. New York, NY: Raven Press; 1977:655–659.

9. van Kammen DP, Bunney WE, Docherty JP, et al. d-amphetamine-induced heterogeneous changes in psychotic behavior in schizophrenia. *Am J Psychiatry.* 1982;139:991–997.

10. Angrist B, Rotrosen J, Gershon S. Response to apomorphine, amphetamine, and neuroleptics in schizophrenic subjects. *Psychopharmacology.* 1980;67:31–38.

11. van Kammen DP, Schulz SC, Rogol AD. Hormonal response to d-amphetamine in schizophrenia. In: Shah ED, Donald AG, eds. *Psychoneuroendocrine Dysfunction in Psychiatry and Neurological Illness: Influence of Pharmacological Agents.* New York, NY: Plenum Press; 1984:163–182.

12. Angrist B, Rotrosen J, Gershon S. Differential effects of amphetamine and neuroleptics on negative vs. positive symptoms in schizophrenia. *Psychopharmacology.* 1980;72:17–19.

13. Schulz SC, van Kammen DP, Rogol AD, et al. Amphetamine increases prolactin but neither growth hormone nor beta-endorphin immunoreactivity in schizophrenic patients. *Psychopharmacol Bull.* 1981;17:193–195.

14. van Kammen DP, Docherty JP, Bunney WE. Prediction of early relapse after pimozide discontinuation by response to d-amphetamine during pimozide treatment. *Biol Psychiatry.* 1982;17:233–242.

15. Angrist B, Peselow E, Rotrosen J, et al. Relationship between responses to dopamine agonists, psychopathology, neuroleptic maintenance in schizophrenic subjects. In: Angrist B, Burrows G, Lader M, eds. *Recent Advances in Neuropsychopharmacology.* Vol 31. New York, NY: Pergamon Press; 1981:49–54.

16. Baxter LR Jr. PET studies of cerebral function in major depression and obsessive-compulsive disorder: the emerging prefrontal cortex consensus. *Ann Clin Psychiatry.* 1991;3:103–109.

17. Devous MD Sr. Imaging brain function by single-photon emission computed tomography. In: Andreasen N, ed. *Brain Imaging: Applications in Psychiatry.* Washington, DC: American Psychiatric Press; 1988:147–234.

18. Spitzer RL, Williams JBW, Gibbons M, et al. Structured clinical interview for DSMIIIR (SCID). I. History and rationale. *Arch Gen Psychiatry.* 1992;49:624–629.

19. Devous MD Sr, Payne JK, Lowe JL. Dual-isotope brain SPECT imaging with ^{99m}Tc and ^{123}I: clinical validation using ^{133}Xe SPECT. *J Nucl Med.* 1992;33:1919–1924.

20. Devous MD Sr, Lowe JL, Payne JK. Dual-isotope brain SPECT imaging with ^{99m}Tc and ^{123}I: validation by phantom studies. *J Nucl Med.* 1992;33:2030–2035.

21. Wechsler LR, Savaki HE, Sokoloff L. Effects of d- and l-amphetamine on local cerebral glucose utilization in the conscious rat. *J Neurochem.* 1979;32:15–22.

22. McCulloch J, Kelly PAT, Ford I. Effect of apomorphine on the relationship between local cerebral glucose utilization and local cerebral blood flow (with an appendix on its statistical analysis). *J Cereb Blood Flow Metab.* 1982;2:487–499.

23. Talairach J, Tournoux P. *Co-Planar Stereotaxic Atlas of the Human Brain.* Stuttgart, Germany: Thieme; 1988.

24. Pelizzari CA, Chen GTY, Spelbring DR, Weichselbaum RR, Chen CT. Accurate three-dimensional correlation of CT, PET and MR images of the brain. *J Comput Assist Tomogr.* 1989;13:20–26.

25. Lamoureux G, Dupont RM, Ashburn WL, et al. "CORT-EX": a program for quantitative analysis of brain SPECT data. *J Nucl Med.* 1990;31:1862–1871.

26. Coyle JT, Snider SH. Catecholamine uptake by synaptosomes in homogenates of rat brain: stereospecificity in different areas. *J Pharm Exp Ther.* 1969;170:221–231.

27. Bunney BS, Walters JR, Kuhar MJ, et al. d- and l-amphetamine stereoisomers: comparative potencies in affecting the firing of central dopaminergic and noradrenergic neurons. *Psychopharmacol Commun.* 1975;1:177–190.

28. Philips AG, Fibiger HC. The role of dopamine in maintaining intracranial self-stimulation in the ventral tegmentum, nucleus accumbens, and prefrontal cortex. *Can J Psychol.* 1978;32:58–66.

29. Lyness WH, Friedle NM, Moore KE. Destruction of dopaminergic terminals in nucleus accumbens: effect on d-amphetamine self-administration. *Pharm Biochem Behav.* 1979;11:553–556.

30. Antelman SM, Chiodo LA. Dopamine autoreceptor subsensitivity: a mechanism common to the treatment of depression and the induction of amphetamine psychosis. *Biol Psychiatry.* 1981;16:717–725.

31. Woolverton WL, Balster RL Behavioral pharmacology of local anaesthetics: reinforcing and discriminative stimulus effects. *Pharmacol Biochem Behav.* 1982;16:491–500.

32. Taylor KM, Snyder SH. Differential effects of d- and l-amphetamine on behavior and on catecholamine disposition in dopamine and norepinephrine containing neurons of rat brain. *Brain Res.* 1971;28:295–309.

33. Alexander GE, Crutcher MD, DeLong MR. Basal ganglia-thalamocortical circuits: parallel substrates for motor, oculomotor, "pre-frontal" and "limbic" functions. In: Uylings HBM, Van Eden CG, De Vruin JPC, Corner MA, Feenstra MGP, eds. *Progress in Brain Research.* Vol 85. New York, NY: Elsevier Science Publishers; 1990:119–146.

34. Mega MS, Cummings JL. Frontal-subcortical circuits in neuropsychiatric disorders. *J Neuropsychiatry Clin Neurosci.* 1994;6:358–370.

35. Kapur S, Mann JJ. Role of the dopaminergic system in depression. *Biol Psychiatry.* 1992;32:1–17.

36. Wolkin A, Angrist B, Wolf A, et al. Effects of amphetamine on local cerebral metabolism in normal and schizophrenic subjects as determined by positron emission tomography. *Psychopharmacology.* 1987;92:241–246.

37. Wolkin A, Sanfilipo M, Angrist B, et al. Acute d-amphetamine challenge in schizophrenia: effects on cerebral glucose utilization and clinical symptomatology. *Biol Psychiatry.* 1994;36:317–325.

38. Daniel DG, Weinberger DR, Jones DW, et al. The effect of amphetamine on regional cerebral blood flow during cognitive activation in schizophrenia. *J Neurosci.* 1991;11:1907–1917.

39. Mattay VS, Berman KF, Ostrem JL, et al. Dextroamphetamine enhances "neural network-specific" physiological signals: a positron-emission tomography rCBF study. *J Neurosci.* 1996;16:4816–4822.

40. Matochik JA, Nordahl TE, Gross M, et al. Effects of acute stimulant medication on cerebral metabolism in adults with hyperactivity. *Neuropsychopharmacology.* 1993;8:377–386.

41. Ernst M, Zametkin AJ, Matohik JA, et al. Effects of intravenous dextroamphetamine on brain metabolism in adults with attention-deficit hyperactivity disorder (ADHD): preliminary findings. *Psychopharm Bull.* 1994;30:219–225.

Erratum

There was a typographical error in the title of the article, "Reproducibility of Renal Length Measurements with ^{99m}Tc-DSMA SPECT," by Lin et al. (*JNM* 2000;41:1632–1635). It should have read, "Reproducibility of Renal Length Measurements with ^{99m}Tc-DMSA SPECT." We regret the error.